Electronic Supplementary Material (ESI) for Journal of Materials Chemistry A.

Supplementary Information

Phase Controllable Synthesis of Three-Dimensional Star-like MnO_2 Hierarchical Architectures as Highly Efficient and Stable Oxygen Reduction Electrocatalysts

Gao Cheng,[a] Shilei Xie,[b] Bang Lan,[c] Xiaoying Zheng,[a] Fei Ye,[a] Ming Sun,[a] Xihong Lu[b]* and Lin Yu[a]*

[a]Key Laboratory of Clean Chemistry Technology of Guangdong Regular Higher Education Institutions, School of Chemical Engineering and Light Industry, Guangdong University of Technology, Guangzhou 510006, P. R. China.

E-mail: gych@gdut.edu.cn (Lin Yu).

[b]MOE of the Key Laboratory of Bioinorganic and Synthetic Chemistry, School of Chemistry and Chemical Engineering, Sun Yat-Sen University, Guangzhou 510275, P. R. China.

E-mail: luxh6@mail.sysu.edu.cn (Xihong Lu).

[c]GuangDong MeiZhou Quality & Metrology Supervision and Testing Institution, Meizhou 514072, P. R. China.

Experimental Section

Controlled Synthesis of Manganese Dioxides

$Mn(CH_3COO)_2$ was reacted with $XClO_3$ (X = K, Na) under acidic conditions to synthesize 3D star-like manganese dioxides with different crystal structures. α-MnO_2 products were synthesized in the following way: A volume of 1.0 mL of condensed CH_3COOH was added into 15 mL of deionized (DI) water. The diluted CH_3COOH solution was then poured into a 25 mL Teflon liner containing stoichiometric mixtures composed of 1 mmol $Mn(CH_3COO)_2$ and 1.75 mmol $KClO_3$ under vigorous stirring at room temperature for half an hour. The Teflon liner was sealed in a stainless steel autoclave and hydrothermally heated in an oven at 160 °C for 12 h. After cooling to room temperature, the solid products were centrifuged with DI water and absolute ethanol to remove impurities, and dried overnight in air at 60 °C. ε-MnO_2 products can be conveniently prepared by following the above synthesis procedure except changing the $KClO_3$ as $NaClO_3$. The commercial MnO_2 (bulk MnO_2) was purchased from Sinopharm Chemical Reagent Co., Ltd. All chemicals reagents were used without further purification.

To investigate the effects of various reaction parameters on the morphology of the MnO_2 products, a series of control experiments were carried out by altering the reaction parameters, which were summarized as follows:

1) Effects of the reaction temperature: the precursor solutions were treated at different reaction temperatures (120, 140 and 180 °C) with other reaction parameters unchanged.

2) Effects of the anion type: (a) SO_4^{2-}:1 mmol $MnSO_4{\cdot}H_2O$ and 1.0 ml of condensed H_2SO_4, (b) Cl^-: 1 mmol $MnCl_2{\cdot}4H_2O$ and 1.5 ml of condensed HCl and (c) NO_3^-: 1 mmol $Mn(NO_3)_2{\cdot}6H_2O$

and 1.1 ml of condensed HNO_3, respectively, were reacted with $XClO_3$ (X = K, Na) while keeping the other synthetic conditions.

3) Effects of the reaction time: time-dependent experiments (60, 90, 150 and 480 min) were performed using the above synthesis procedures with other reaction parameters unchanged.

Materials Characterization

X-ray powder diffraction (XRD) was performed on a Brucker D8 X-ray diffractometer operating at a voltage of 40 kV and a current of 40 mA with Cu Kα radiation. The data were collected at room temperature with a 0.01° step size in 2θ, from $2\theta = 10$ to 80°. The field emission scanning electron microscopy (FESEM) images were taken on a ZEISS Ultra 55 instrument. The transmission electron microscopy (TEM), high-resolution transmission electron microscopy (HRTEM) and selected area electron diffraction (SAED) patterns were recorded on a JEOL JEM-2100HR at an acceleration voltage of 200 kV. X-ray photoelectron spectroscopy (XPS) was recorded on a Thermo ESCALAB 250 instrument equipped with a monochromatic Al Kα (1486.6 eV) X-ray source. The instrument was operated at 150 W with a spot size of 500 μm in diameter. The spectra are calibrated using the carbon peak. The BET surface areas of the obtained products were measured by a multipoint N_2 adsorption-desorption method in liquid N_2 (196 °C) with a GEMINI V 2380 surface area analyzer. Samples were treated under 150 °C in N_2 atmosphere for 8 h to evacuate the physisorbed moisture before measurement. For the O_2 temperature-programmed desorption (O_2-TPD) experiment, about 30 mg samples were loaded in a U-shaped quartz micro-reactor. After being pretreated in flowing He at 250 °C for 1 h and cooled to room temperature, the samples were exposed to O_2 atmosphere for 20 min, and subsequently heated to 800 °C at a heating rate of 10 $^{o}C\ min^{-1}$ in flowing He.

Electrochemical measurements

The electrochemical measurements were performed with a three-electrode system in 0.1 M KOH aqueous solution, which was saturated with high-purity N_2 or O_2 for at least 30 min prior to each test and maintained under N_2 or O_2 atmosphere through the whole test. The reference electrode was an Ag/AgCl in 3.5 M KCl solution and the counter electrode was a Pt foil. The working electrode was a sample-coated glassy carbon (GC) electrode, which is confined in a rotating ring-disk electrode (RRDE, Pt ring and GC disk, disk diameter 5.61 mm). 5 mg of the catalyst (containing the as-prepared MnO_2 samples and carbon powders (Ketjenblack) at a 3:7 mass ratio) was ultrasonically dispersed in the 1.0 mL of mixed solvent that contained 950 μL isopropyl alcohol and 50 μL neutralized Nafion solution (5 wt%, DuPont) for 30 min to form a homogeneous ink. Then, 5.0 μL of the catalyst ink was loaded onto the GC electrode and naturally dried under air atmosphere to allow solvent evaporation. Cyclic voltammograms (CVs) and linear sweep voltammograms (LSVs) were carried out at room temperature on the computer-controlled CHI 760E bipotentiostats assembled with a rotating system (GAMRY RDE710). The scan rate of CVs was kept as 50 mV s^{-1} while that for LSVs was 5 mV s^{-1}. The disk electrode was scanned cathodically at a rate of 5 mV s^{-1} and the Pt ring potential was constant at 0.6 V to monitor any peroxide (HO_2^-) species. The conductivity of the as-prepared MnO_2 samples is measured by two-point current-potential (I-V) curves by a typical two electrode system (ZAHNER, Germany) at room temperature. All the potentials were transferred to the RHE potential scale, and the following equation was used:

$$E_{RHE} = E_{AgCl} + 0.059\ \mathrm{pH} + E^{0}_{AgCl}$$

where E_{RHE} is the applied potential vs. RHE, E_{AgCl} is the applied potential vs. Ag/AgCl and $E0$ AgCl is the standard potential of the Ag/AgCl reference electrode.

The ORR kinetics was analyzed by the Koutecky-Levich (K-L) equation:[1]

$$\frac{1}{J} = \frac{1}{J_L} + \frac{1}{J_K} = \frac{1}{0.62nFC_0(D_0)^{2/3}(v)^{-1/6}\omega^{1/2}} + \frac{1}{nFkC_0}$$

where J is the measured current density, J_K and J_L are the kinetic- and diffusion-limiting current densities, ω is the angular velocity of the disk, n is the number of electrons transferred in the oxygen reduction, F is the Faraday constant ($F = 96\,485$ C mol^{-1}), C_0 is the bulk concentration of O_2 ($C_0 = 1.2 \times 10^{-6}$ mol cm^{-3}), D_0 is the diffusion coefficient ($D_0 = 1.9 \times 10^{-5}$ cm^2 s^{-1}). v is the kinematic viscosity of the electrolyte ($v = 0.01$ cm^2 s^{-1}), and k is the electron-transfer rate constant.

The peroxide yields (y_{peroxide}) and the electron transfer number (n) were determined by the following equations:[2]

$$y_{peroxide} = 200\frac{I_r/N}{I_d + I_r/N}$$

$$n = 4\frac{I_d}{I_d + I_r/N}$$

where I_r is the ring current, I_d is the disk current, N is the current collection efficiency of the RRDE.

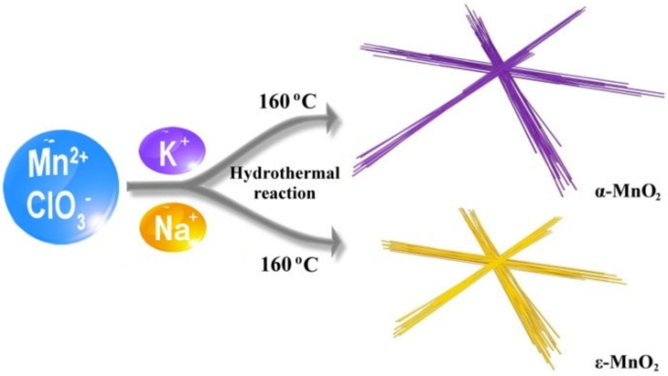

Fig. S1 Schematic illustration of the preparation of 3D MnO_2 star-like hierarchical architectures.

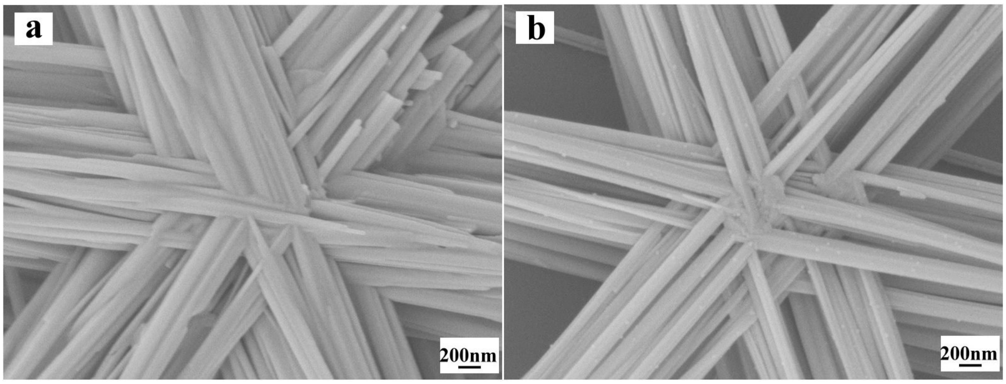

Fig. S2 High-magnification FESEM images of the central part for (a) α-MnO_2 and (b) ε-MnO_2 samples.

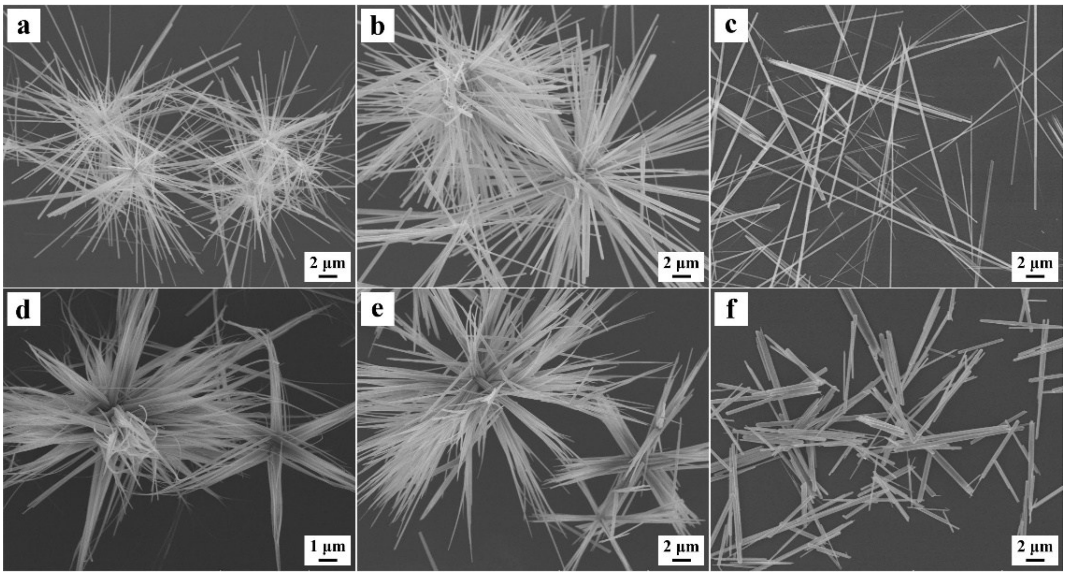

Fig. S3 FESEM images of the MnO_2 products prepared at different reaction temperatures by using $KClO_3$ (a-c) or $NaClO_3$ (d-f) as the oxidants: (a, d) 120 °C, (b, e) 140 °C and (c, f) 180 °C.

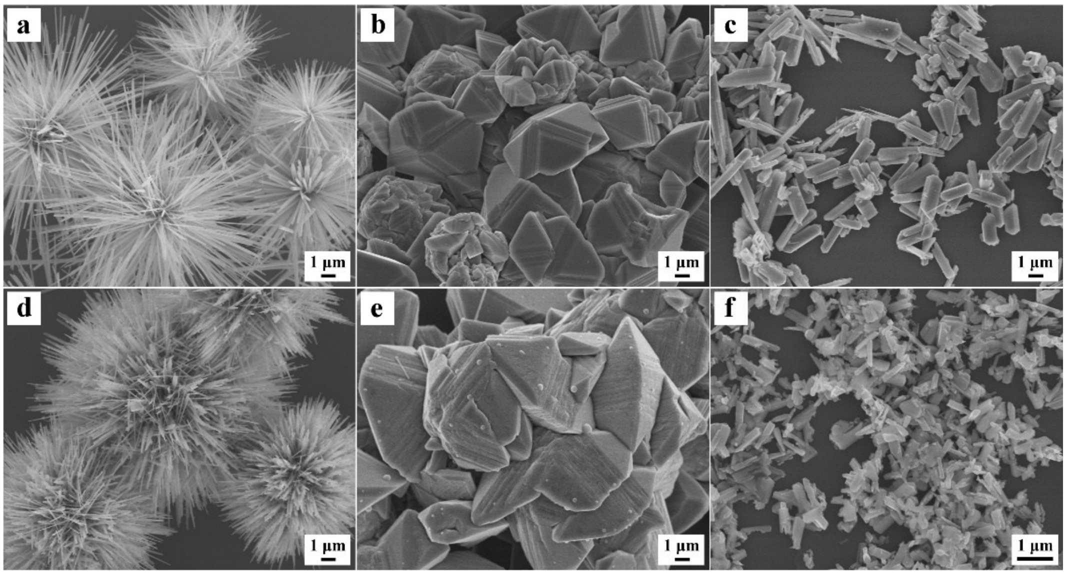

Fig. S4 FESEM images of the MnO_2 products prepared by different kinds of anions using $KClO_3$ (a-c) or $NaClO_3$ (d-f) as the oxidants: (a, d) SO_4^{2-}, (b, e) Cl^- and (c, f) NO_3^-.

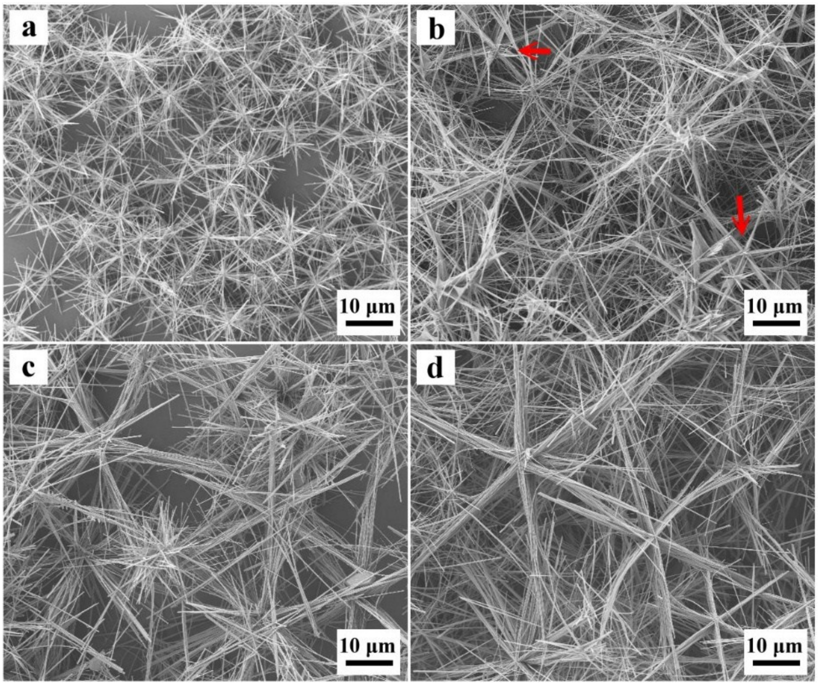

Fig. S5 FESEM images of the α-MnO_2 hierarchical stars prepared at different reaction times: (a) 60 min; (b) 90 min; (c) 150 min; (d) 480 min.

At 60 min, the urchin-like MnO_2 nanostructures formed of nanorods can be clearly observed, which have a diameter of ~ 10 μm (Fig. S5a). After 90 min, the nanorods originating from the core of the urchin-like MnO_2 nanostructures are changed into nanowires with a length of ~ 20 μm (Fig S5b), and the MnO_2 star-like hierarchical architectures start to appear (indicated with an arrow). After 150 min, the morphology of the as-obtained products change markedly. A large number of α-MnO_2 star-like nanostructures with six branches are formed (Fig. S5c). After a 480 min reaction, the products consist predominantly of 3D α-MnO_2 star-like nanostructures (Fig. S5d).

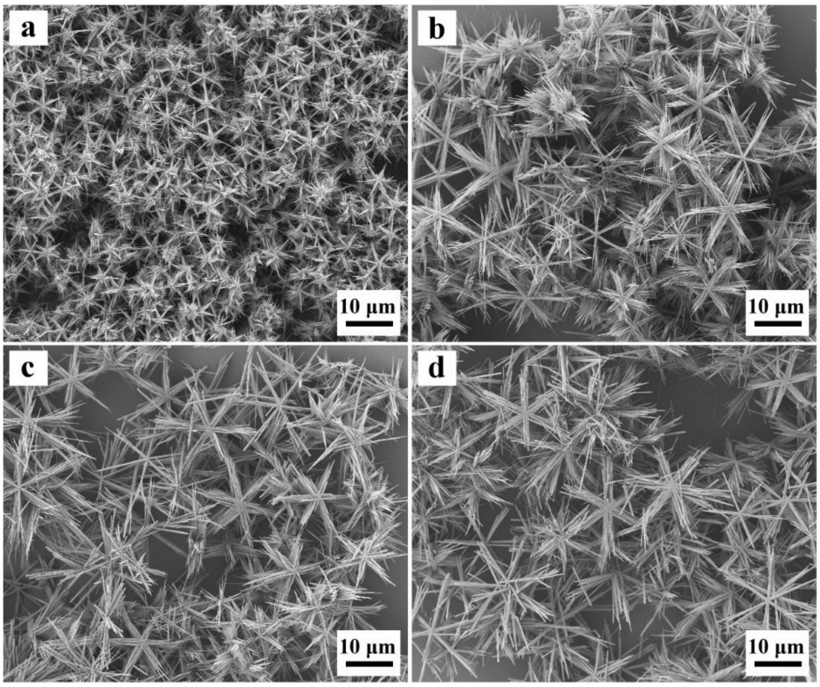

Fig. S6 FESEM images of the ε-MnO_2 hierarchical stars prepared at different reaction times: (a) 60 min; (b) 90 min; (c) 150 min; (d) 480 min.

At 60 min, many small MnO_2 3D nanostructures are formed, which have an average size of ~ 6 μm (Fig. S6a). After 90 min, the ε-MnO_2 star-like hierarchical architectures with a large average size of ~13 μm can be observed (Fig. S6b). Further increasing the reaction time (150 min and 480 min) results in the growth of larger 3D ε-MnO_2 star-like hierarchical architectures (Fig. S6c and Fig. S6d).

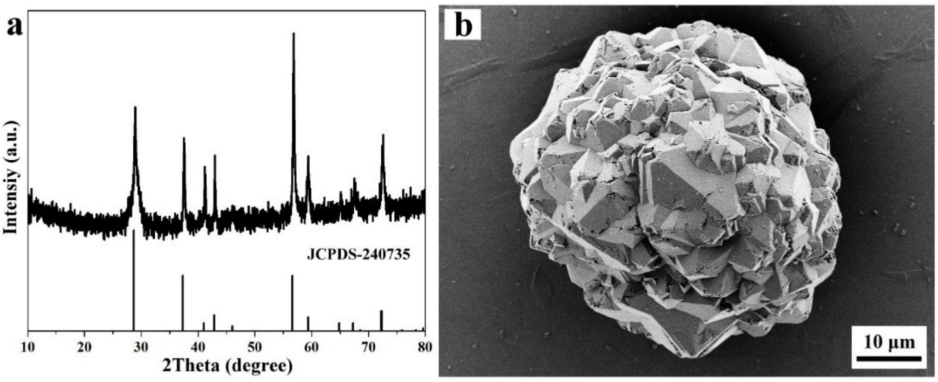

Fig. S7 (a) XRD pattern and (b) FESEM images of the commercial MnO_2.

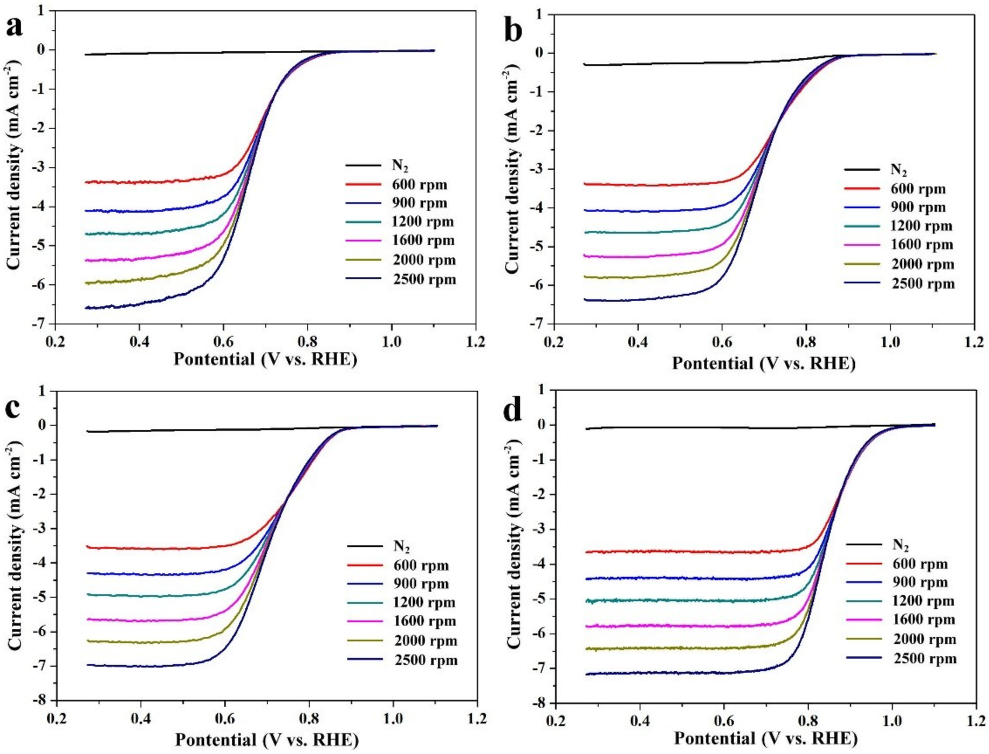

Fig. S8 LSV curves of (a) bulk MnO_2, (b) ε-MnO_2, (c) α-MnO_2 and (d) Pt/C at different rotation speeds recorded in N_2- and O_2-saturated 0.1 M KOH solution.

Table R1 Electrocatalytic performances (E_{onset} and $E_{1/2}$) of recently reported non-noble metal catalysts

Samples	E_{onset} (V)	$E_{1/2}$ (V)	Ref
α-MnO_2 hierarchical stars	0.84	0.72	This work
α-MnO_2 nanowires	0.80	0.56	3
Mn_2O_3 nanoballs	0.82	0.68	4
Cu-α-MnO_2 nanowires	0.85	0.71	5
α-MnO_2 nanoparticles	0.71	0.57	6
MnO_2 nanoflakes	0.82	0.67	7
β-MnO_2 nanorods with vacanices	0.86	0.72	8
mesoporous $CuCo_2O_4$ nanoparticles	0.87	0.51	9
Cr_2O_3/ reduced graphene oxides	0.68	0.62	10
urchin-like CoP	0.80	0.70	11
$MnCo_2O_4$ nanofibres	0.82	0.70	12
Co_3O_4 nano-octahedrons/ reduced graphene oxides	0.82	0.68	1

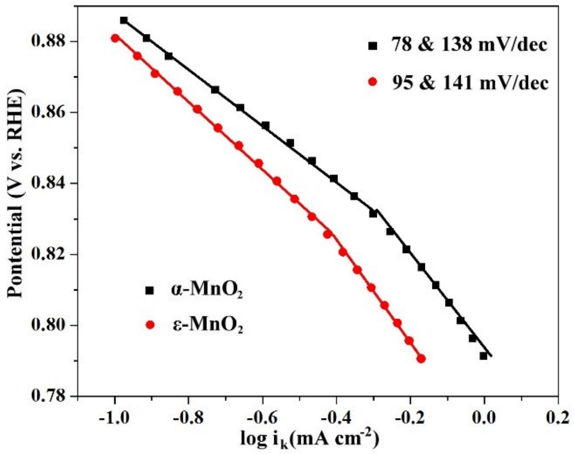

Fig. S9 Tafel plots derived from the corresponding voltammetry data.

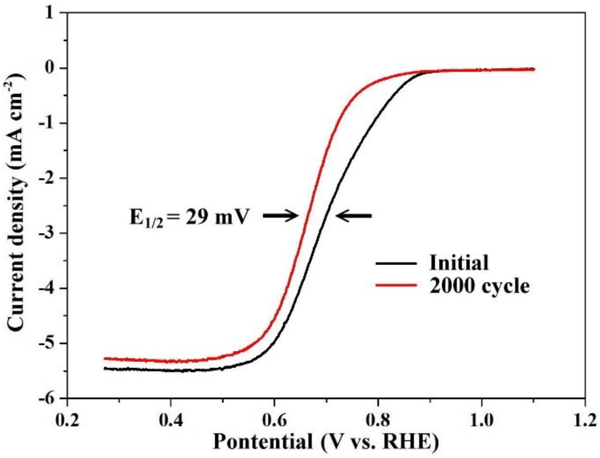

Fig. S10 LSV curves of the α-MnO_2 hierarchical stars before and after 2000 CV cycles.

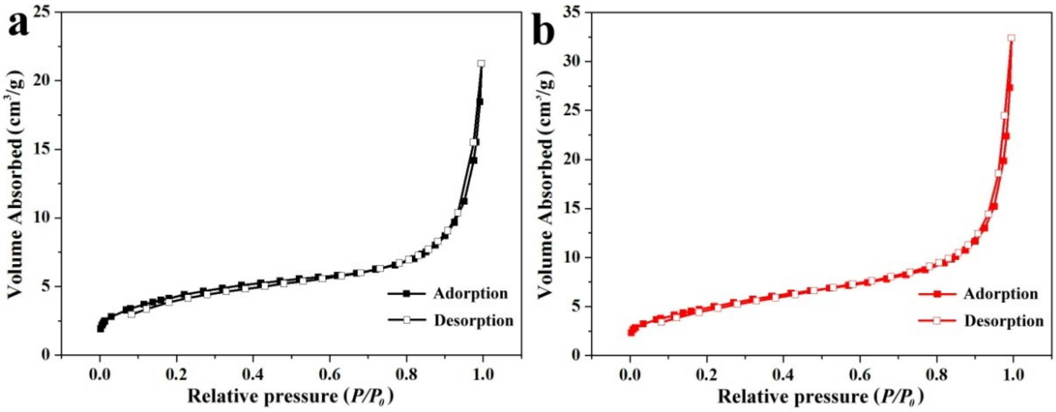

Fig. S11 The typical N_2 adsorption-desorption isotherms of the (a) α-MnO_2 and (b) ε-MnO_2 samples.

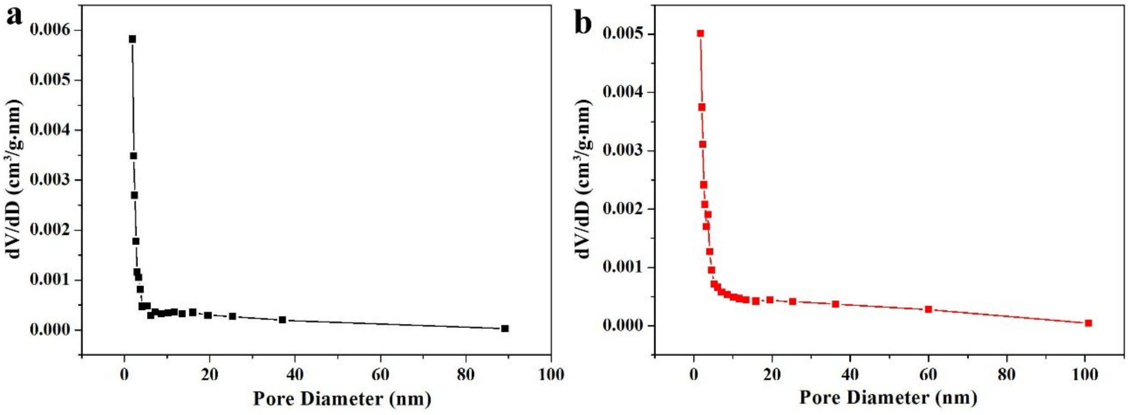

Fig. S12 Pore size distribution from the desorption branch of the (a) α-MnO_2 and (b) ε-MnO_2.

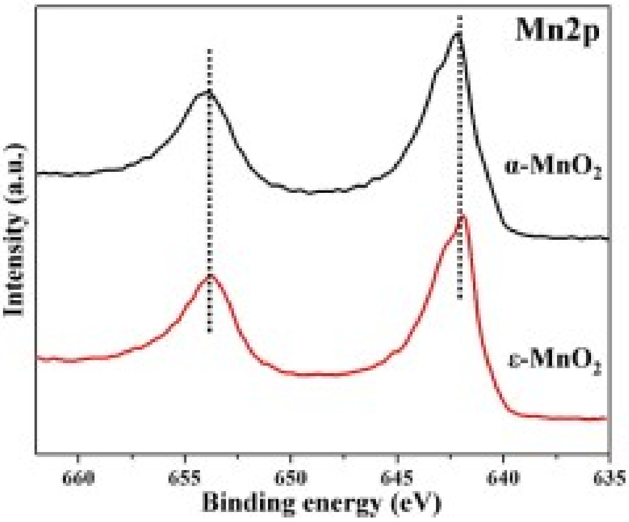

Fig. S13 XPS spectra of Mn 2p for α-MnO_2 and ε-MnO_2 samples.

References

1 J. Xiao, Q. Kuang, S. Yang, F. Xiao, S. Wang and L. Guo, *Sci. Rep.*, 2013, **3**, 2300.

2 T. Zhang, F. Cheng, J. Du, Y. Hu and J. Chen, *Adv. Energy. Mater.*, 2015, **5**, 1400654.

3 M. Lehtimäki, H. Hoffmannová, O. Boytsova, Z. Bastl, M. Busch, N. B. Halck, J. Rossmeisl and P. Krtil, *Electrochim. Acta*, 2016, **191**, 452.

4 S. Ghosh, P. Kar, N. Bhandary, S. Basu, S. Sardar, T. Maiyalagan, D. Majumdar, S. K. Bhattacharya, A. Bhaumik, P. Lemmens and S. K. Pal, *Catal. Sci. Technol.*, 2016, **6**, 1417.

5 D. J. Davis, T. N. Lambert, J. A. Vigil, M. A. Rodriguez, M. T. Brumbach, E. N. Coker and S. J. Limmer, *J. Phys. Chem. C*, 2014, **118**, 17342.

6 C. Shi, G.-L. Zang, Z. Zhang, G.-P. Sheng, Y.-X. Huang, G.-X. Zhao, X.-K. Wang and H.-Q. Yu, *Electrochim. Acta*, 2014, **132**, 239.

7 C. Wei, L. Yu, C. Cui, J. Lin, C. Wei, N. Mathews, F. Huo, T. Sritharan and Z. Xu, *Chem. Commun.*, 2014, **50**, 7885.

8 F. Cheng, T. Zhang, Y. Zhang, J. Du, X. Han and J. Chen, *Angew. Chem., Int. Ed.*, 2013, **52**, 2474.

9 P.-X. Wang, L. Shao, N.-Q. Zhang and K.-N. Sun, *J. Power Sources*, 2016, **325**, 506.

10 Wen, X. Gao, T. Huang, X. Wu, L. Xu, J. Yu, H. Zhang, Z. Zhang, J. Han and H. Ren, *Int. J. Hydrogen Energy*, 2016, **41**, 11099.

11 H. Yang, Y. Zhang, F. Hu and Q. Wang, *Nano letters*, 2015, **15**, 7616.

12 K. N. Jung, S. M. Hwang, M. S. Park, K. J. Kim, J. G. Kim, S. X. Dou, J. H. Kim and J. W. Lee, *Sci. Rep.*, 2015, **5**, 7665.